CAD/CAM of Orthogonal and Angle-Interlock Woven Structures for Industrial Applications

X. CHEN AND P. POTIYARAJ

Department of Textiles, University of Manchester Institute of Science and Technology, Manchester, M60 1QD, United Kingdom

ABSTRACT

As a continuation of our previous work, this paper concentrates on two more complex 3D woven structures, *i.e.*, orthogonal and angle-interlock structures, for industrial applications such as textile composites. Studying the features of these woven structures has led to the establishment of mathematical models to describe them. Further, algorithms for generating these weave structures are developed based on these models. A CAD/CAM software for these 3D woven structures is created on the MS Windows platform. Solid models of the structures are also made available using virtual reality modeling language (VRML).

High performance woven textile structures have been widely used in developing various innovative materials, of which textile reinforced composites and geotextiles are examples. In order to achieve specific properties, high performance woven textiles have complicated 3D woven structures such as multilayer, orthogonal, and angle-interlock structures, which add extra difficulty to their design and manufacture. CAD/CAM systems for woven structures such as ScotWeave and Sophis are commercially available to assist the design and manufacture of a wide range of woven structures. Unfortunately, these commercial systems, to our best knowledge, do not include facilities for the CAD/CAM of the complicated 3D structures we discuss here.

Research work (including our own) attempting to model intricate weaves and develop algorithms for the CAD/CAM of complicated woven structures has been going on for years [3–5, 6, 10]. Mathematical models and algorithms have been developed to deal with different kinds of woven structures, among which are backed-cloth and multilayer weaves. Based on the modeling for these woven structures, we have developed modules of a CAD/CAM software package accordingly [5, 6, 10].

In this paper, we will focus on two other complex 3D woven structures, orthogonal and angle-interlock, in an attempt to describe the weaves and create the algorithms for the CAD/CAM of these structures. We will also apply the theory to the establishment of a software module that creates solid models for these structures using a virtual reality modelling language (VRML). These models are useful in visualizing the complicated woven structures and evaluating their physical and other properties.

Orthogonal Structures

There are three sets of yarns in an orthogonal structure, the straight warp yarn, the straight weft yarn, and the binding warp yarn. The straight warp and weft yarns form the non-interlaced body structure that is integrated by the binding warp ends following the binding weave. The thickness of this structure is measured by the number of layers of the straight warp or weft yarn. According to the binding weave, there are two kinds of orthogonal structures, *i.e.*, ordinary and enhanced [4]. An ordinary structure uses only one binding warp set, while an enhanced structure uses two binding warp sets with inverse binding weaves. Figure 1a shows an ordinary orthogonal structure with four layers of straight weft, three layers of straight warp, and a ⅓ twill binding weave. Figure 1b shows an enhanced structure of the same configuration.

The relationship between the number of layers of straight warp N_w and layers of straight weft N_f can be explained as follows [4]:

$$N_f = N_w + 1 \quad . \tag{1}$$

Warp and weft repeats R_e and R_p of an orthogonal structure can be calculated according to the numbers of layers of straight warp and weft and the warp repeat B_e and weft repeat B_p of the binding weave:

$$R_e = (N_w + t) \times B_e \tag{2}$$

and

$$R_p = N_f \times B_p \quad , \tag{3}$$

where $t = 1$ in the case of an ordinary orthogonal structure and 2 in the case of an enhanced orthogonal structure.

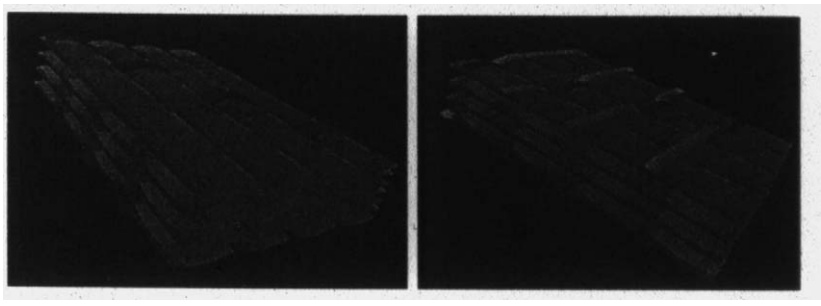

FIGURE 1. (a) An ordinary orthogonal structure, (b) an enhanced orthogonal structure.

Figures 2a and b show the weaves of the orthogonal structures demonstrated in Figure 1. The binding weave and the inverse binding weave are ⅓ and 3/1 "Z" twills, respectively.

As a convention in our earlier papers [5, 6, 10], we used a binary matrix for the mathematical representation of a weave. Each element of the matrix is assigned to either 0 or 1, corresponding to a blank or a mark on the design paper. Figure 3 demonstrates the weave matrix of the binding weave ⅓ Z. A binding weave can be generated by the same weave creation technique used for single layer fabrics; this technique has been explained in detail in our earlier work (Chen *et al.* [3]).

In order to generate an orthogonal weave, it is necessary to provide the number of straight warp layers N_w or straight weft layers N_f, the binding weave, and the kind of orthogonal structure, *i.e.*, ordinary or enhanced. When these parameters are provided, the matrix for the non-interlaced body structure is generated by the following assignment:

If $(x - 1) \bmod N_w < (y - 1) \bmod N_f$ and $1 \le x \le N_w \times B_e$ and $1 \le y \le R_p$,

$$W_{x,y}^{ni} = 1 \quad .$$

Otherwise,

$$W_{x,y}^{ni} = 0 \quad ,$$

where W^{ni} is the weave matrix for the non-interlaced body structure, $W_{x,y}^{ni}$ is the element of matrix W^{ni} at the x^{th} warp and the y^{th} weft, and "mod" refers to a modulus division that returns only the remainder of the division. For example, 5 mod 3 returns 2.

The binding weave is introduced to integrate the non-interlaced body structure. Weft repeats of the binding weave and the inverse binding weave must be expanded to suit the straight weft repeat before the introduction using the following equation:

$$W_{x,y}^{be} = W_{x,j}^{b} \quad \text{for } 1 \le x \le B_e \text{ and } 1 \le y \le R_p \quad , \quad (4)$$

where $W_{x,y}^{be}$ is the extended binding weave matrix and $W_{x,j}^{b}$ is binding weave matrix, $j = \{(y - 1) \backslash N_f\} + 1$, and \ is the integral division operator used for dividing two numbers. The result is rounded down and the operation returns an integer. For example, in the expression of $a = 17 \backslash 3$, a is equal to 5.

In the case of an inverse binding weave,

$$W_{x,y}^{ie} = W_{x,j}^{i} \text{ for } 1 \le x \le B_e \text{ and } 1 \le y \le R_p \quad , \quad (5)$$

where $W_{x,y}^{ie}$ is the extended inverse binding weave matrix, $W_{x,j}^{i}$ is the inverse binding weave matrix, and $j = \{(y - 1) \backslash N_f\} + 1$. Then the extended binding weave will be inserted into the non-interlaced body structure Equations 6 and 7 are used for ordinary and enhanced orthogonal structures, respectively:

$$W_{x,y} = \begin{cases} W_{a,y}^{ni} & \text{if } (x - 1) \bmod (nw + 1) > 0 \\ W_{b,y}^{be} & \text{if } (x - 1) \bmod (nw + 1) = 0 \end{cases}$$

$$\text{for every } 1 \le x \le Re \quad \text{and} \quad 1 \le y \le Rp \quad , \quad (6)$$

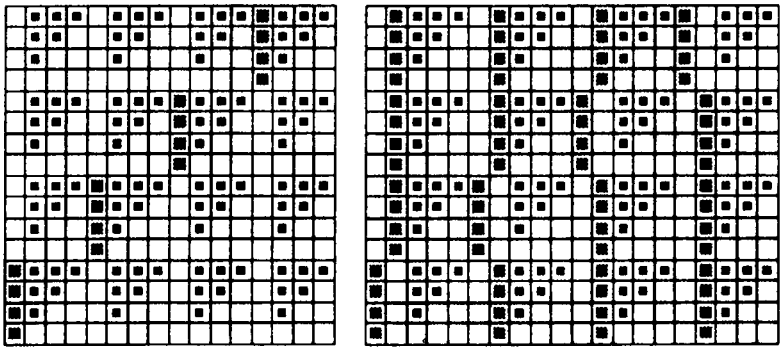

FIGURE 2. (a) An ordinary orthogonal weave, (b) an enhanced orthogonal weave.

$$\begin{bmatrix} 0 & 0 & 0 & 1 \\ 0 & 0 & 1 & 0 \\ 0 & 1 & 0 & 0 \\ 1 & 0 & 0 & 0 \end{bmatrix}$$

FIGURE 3. Weave matrix of the binding weave ⅓ "Z."

where $a = \{[(x-1)\backslash(N_w+1)]*N_w\} + [(x-1) \bmod (N_w+1)]$, and $b = [(x-1)\backslash(N_w+1)] + 1$.

$$W_{x,y} = \begin{cases} W_{a,y}{}^{ni} & \text{if } (x-1) \bmod (nw+2) > 0 \\ W_{b,y}{}^{be} & \text{if } (x-1) \bmod (nw+2) = 0 \\ W_{b,y}{}^{ie} & \text{if } (x-1) \bmod (nw+2) = 1 \end{cases}$$

$$\text{for every } \quad 1 \le x \le Re \quad \text{and} \quad 1 \le y \le R \quad , \qquad (7)$$

where $a = [\{(x-1)\backslash(N_w+2)\}*N_w] + \{(x-2) \bmod (N_w+2)\}$, $b = \{(x-1)\backslash(N_w+2)\} + 1$, and $c = \{(x-2)\backslash(N_w+2)\} + 1$.

Take Figure 2a as an example to illustrate the procedure. This is an ordinary orthogonal weave with $N_w = 3$ and ⅓ twill as the binding weave. Therefore,

$$N_w = 3 \quad N_f = 4$$

$$B_e = 4 \quad B_p = 4 \quad t = 1$$

The warp and weft repeats of this ordinary orthogonal weave are then

$$R_e = (3+1) \times 4 = 16 \quad \text{and} \quad R_p = 4 \times 4 = 16 \quad .$$

From the parameters provided, we can create the matrix W^{ni} for the non-interlaced body structure. For example,

$$W_{1,1}{}^{ni} = 0 \quad \text{as } (1\text{-}1) \bmod 3 = (1\text{-}2) \bmod 4$$

$$W_{1,2}{}^{ni} = 1 \quad \text{as } (1\text{-}1) \bmod 3 < (2\text{-}1) \bmod 4 \quad .$$

The resulting matrix is shown in Figure 4.

Using Equation 4, the number of rows of the binding weave matrix W^b is made equal to R_p, resulting in the extended binding weave matrix W^{be} shown in Figure 5. For example, for the element at $x = 1$ and $y = 2$,

$$j = \{(2\text{-}1)\backslash 4\} + 1 = 1, \text{ hence } W_{1,2}{}^{be} = W_{1,1}{}^{b} \quad .$$

W^{ni} and W^{be} are then merged using Equation 6. The final weave matrix is generated as shown in Figure 6, which represents the weave illustrated in Figure 1a.

$$W^{ni} = \begin{bmatrix} 1&1&1&1&1&1&1&1&1&1&1&1 \\ 1&1&0&1&1&0&1&1&0&1&1&0 \\ 1&0&0&1&0&0&1&0&0&1&0&0 \\ 0&0&0&0&0&0&0&0&0&0&0&0 \\ 1&1&1&1&1&1&1&1&1&1&1&1 \\ 1&1&0&1&1&0&1&1&0&1&1&0 \\ 1&0&0&1&0&0&1&0&0&1&0&0 \\ 0&0&0&0&0&0&0&0&0&0&0&0 \\ 1&1&1&1&1&1&1&1&1&1&1&1 \\ 1&1&0&1&1&0&1&1&0&1&1&0 \\ 1&0&0&1&0&0&1&0&0&1&0&0 \\ 0&0&0&0&0&0&0&0&0&0&0&0 \\ 1&1&1&1&1&1&1&1&1&1&1&1 \\ 1&1&0&1&1&0&1&1&0&1&1&0 \\ 1&0&0&1&0&0&1&0&0&1&0&0 \\ 0&0&0&0&0&0&0&0&0&0&0&0 \end{bmatrix}$$

FIGURE 4. Weave matrix of the straight component of the structure example.

$$W^{be} = \begin{bmatrix} 0&0&0&1 \\ 0&0&0&1 \\ 0&0&0&1 \\ 0&0&0&1 \\ 0&0&1&0 \\ 0&0&1&0 \\ 0&0&1&0 \\ 0&0&1&0 \\ 0&1&0&0 \\ 0&1&0&0 \\ 0&1&0&0 \\ 0&1&0&0 \\ 1&0&0&0 \\ 1&0&0&0 \\ 1&0&0&0 \\ 1&0&0&0 \end{bmatrix}$$

FIGURE 5. Extended binding weave matrix of the structure example.

Angle-Interlock Structures

In an angle-interlock structure, warp yarns are interlocked through several weft yarns in the thickness direction. Variations in the geometry of angle-interlock structures can be achieved by varying the number of weft yarn layers and varying the way the weft yarns are interlocked by the warp ends. We have used the notation $[N_f, N_{ft}]$ to identify angle-interlock structures, where N_f is the number of weft layers and N_{ft} is the number of weft layers interlocked by the warp ends [7]. Naturally, N_f is always larger than or equal to N_{ft}. Figure 7 shows three variations of the angle-interlock structures.

The interlocking warp yarns diagonally interlace with weft yarns in order to obtain an integrated structure and to avoid the excessive curvature of warp yarns. It is unnecessary that all warp yarns interlock weft yarns in the same way. For example, in the *[7, 5]* structure in Figure 7, some warp yarns just interlace with one weft yarn in the thickness direction, while others interlock with weft yarns five layers up or down.

$$W = \begin{bmatrix}
0 & 1 & 1 & 1 & 0 & 1 & 1 & 1 & 0 & 1 & 1 & 1 & 1 & 1 & 1 & 1 \\
0 & 1 & 1 & 0 & 0 & 1 & 1 & 0 & 0 & 1 & 1 & 0 & 1 & 1 & 1 & 0 \\
0 & 1 & 0 & 0 & 0 & 1 & 0 & 0 & 0 & 1 & 0 & 0 & 1 & 1 & 0 & 0 \\
0 & 0 & 0 & 0 & 0 & 0 & 0 & 0 & 0 & 0 & 0 & 0 & 1 & 0 & 0 & 0 \\
0 & 1 & 1 & 1 & 0 & 1 & 1 & 1 & 1 & 1 & 1 & 1 & 0 & 1 & 1 & 1 \\
0 & 1 & 1 & 0 & 0 & 1 & 1 & 0 & 1 & 1 & 1 & 0 & 0 & 1 & 1 & 0 \\
0 & 1 & 0 & 0 & 0 & 1 & 0 & 0 & 1 & 1 & 0 & 0 & 0 & 1 & 0 & 0 \\
0 & 0 & 0 & 0 & 0 & 0 & 0 & 0 & 1 & 0 & 0 & 0 & 0 & 0 & 0 & 0 \\
0 & 1 & 1 & 1 & 1 & 1 & 1 & 1 & 0 & 1 & 1 & 1 & 0 & 1 & 1 & 1 \\
0 & 1 & 1 & 0 & 1 & 1 & 1 & 0 & 0 & 1 & 1 & 0 & 0 & 1 & 1 & 0 \\
0 & 1 & 0 & 0 & 1 & 1 & 0 & 0 & 0 & 1 & 0 & 0 & 0 & 1 & 0 & 0 \\
0 & 0 & 0 & 0 & 1 & 0 & 0 & 0 & 0 & 0 & 0 & 0 & 0 & 0 & 0 & 0 \\
1 & 1 & 1 & 1 & 0 & 1 & 1 & 1 & 0 & 1 & 1 & 1 & 0 & 1 & 1 & 1 \\
1 & 1 & 1 & 0 & 0 & 1 & 1 & 0 & 0 & 1 & 1 & 0 & 0 & 1 & 1 & 0 \\
1 & 1 & 0 & 0 & 0 & 1 & 0 & 0 & 0 & 1 & 0 & 0 & 0 & 1 & 0 & 0 \\
1 & 0 & 0 & 0 & 0 & 0 & 0 & 0 & 0 & 0 & 0 & 0 & 0 & 0 & 0 & 0
\end{bmatrix}$$

FIGURE 6. Weave matrix corresponding to the graphic presentation shown in Figure 1a.

Byun and Chou [2] report that the number of weft layers and the interlocking depth, N_f and N_{ft}, respectively, must be odd numbers and must be larger than three. We have found that the values of N_f and N_{ft} can also be specified as even numbers, leading to perfectly valid angle-interlock structures. However, in such cases, N_f must be made equal to N_{ft}. Figure 7b shows such an example.

In general, the warp ends in the angle-interlock structures can be divided into two groups, *i.e.*, the interlocking and the non-interlocking warp ends. The interlocking warp ends refer to those that interlock through N_{ft} weft layers, while non-interlocking warp ends cover the ones that don't. The numbers of overall, interlocking, and non-interlocking warp ends, denoted by N_w, N_{wi}, and N_{wn}, respectively, can be calculated as follows:

$$N_w = N_f + 1 \quad . \tag{8}$$

$$N_{wi} = \begin{cases} k \times (N_{ft} + 1) & \text{if } k \neq [(N_f + 1)/(N_{ft} + 1)] \\ \left(k - \frac{1}{2}\right) \times (N_{ft} + 1) & \\ \quad \text{if } k = [(N_f + 1)/(N_{ft} + 1)] \text{ and } N_f \neq N_{ft}, & \\ N_w \text{ if } k = [(N_f + 1)/(N_{ft} + 1)] \text{ and } N_f = N_{ft} & \end{cases} \tag{9}$$

$$N_{wn} = N_f - N_{wi} + 1 \quad , \tag{10}$$

where $k = (N_f + 1)\backslash(N_{ft} + 1)$.

Equations 12 and 13 are used to calculate warp repeat R_e and weft repeat R_p of angle-interlock weaves:

$$R_e = N_w \tag{11}$$

and

$$R_p = N_f \times (N_{ft} + 1) \quad . \tag{12}$$

The matrix representing the angle-interlock weave structure W can be generated from the structural parameters, N_f and N_{ft}, and the aforementioned calculated parameters. The element at the x^{th} warp and the y^{th} weft, $W_{x,y}$, is assigned using the following equation:

$$W_{x,y} = \begin{cases} 1; & (y-1)\backslash N_f \leq M_{[(y-1) \bmod N_f],x} \\ 0; & (y-1)\backslash N_f > M_{[(y-1) \bmod N_f],x} \end{cases} \quad \text{for}$$

$$x = 1,2,3,\ldots,R_e \quad \text{and} \quad y = 1,2,3,\ldots,R_p \quad . \tag{13}$$

The procedure above can be illustrated by the following example, which generates the *[5, 3]* angle-interlock weave in Figure 7:

$$N_S = 5, \quad N_{ft} = 3, \quad N_w = 5 + 1 = 6 \quad .$$

$N_{wi} = 1 \times (3 + 1) = 4$ as

$$k \neq (5 + 1)/(3 + 1), \; N_{wn} = 5 - 4 + 1 = 2 \quad ,$$

$$R_e = 6, \quad \text{and} \quad R_p = 5 \times 3 = 15 \quad .$$

FIGURE 7. Angle-interlock structures.

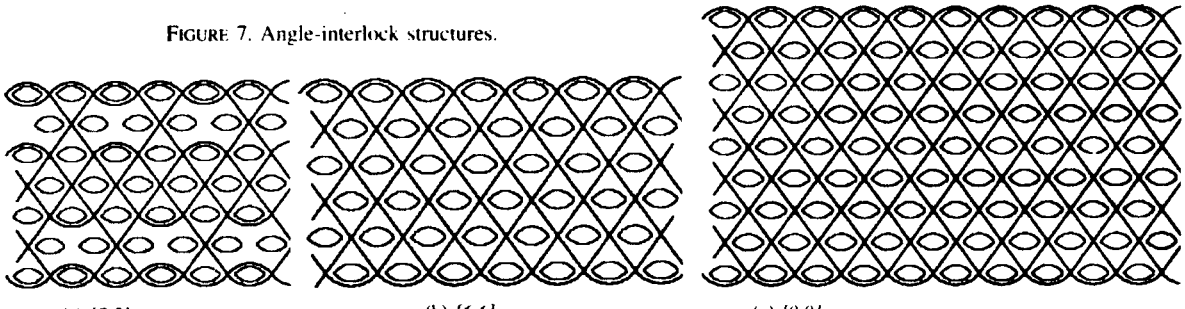

(a) *[7,5]* (b) *[6,6]* (c) *[9,9]*

The weave matrix so generated for the *[5, 3]* angle-interlock structure is shown in Figure 8, which corresponds to the weave, 2D; and 3D representations in Figures 9a, b, and c.

$$W = \begin{bmatrix} 1 & 1 & 1 & 0 & 1 & 0 \\ 1 & 0 & 1 & 0 & 0 & 0 \\ 1 & 1 & 1 & 0 & 1 & 1 \\ 1 & 0 & 1 & 0 & 1 & 0 \\ 0 & 0 & 1 & 0 & 0 & 0 \\ 1 & 1 & 1 & 1 & 0 & 0 \\ 1 & 1 & 0 & 0 & 0 & 0 \\ 1 & 1 & 1 & 1 & 1 & 0 \\ 1 & 1 & 1 & 0 & 0 & 0 \\ 1 & 0 & 0 & 0 & 0 & 0 \\ 1 & 1 & 1 & 1 & 0 & 0 \\ 1 & 1 & 0 & 0 & 0 & 0 \\ 1 & 1 & 1 & 1 & 0 & 1 \\ 1 & 1 & 0 & 1 & 0 & 0 \\ 0 & 1 & 0 & 0 & 0 & 0 \\ 1 & 1 & 1 & 0 & 1 & 0 \\ 1 & 0 & 1 & 0 & 0 & 0 \\ 1 & 1 & 1 & 1 & 1 & 0 \\ 1 & 1 & 1 & 0 & 0 & 0 \\ 1 & 0 & 0 & 0 & 0 & 0 \end{bmatrix}$$

FIGURE 8. Weave matrix generated from the example.

Draft and Lifting Plans

We have successfully applied CAM technology to the weaving of complex structures. It involves the generation of instruction codes to control the shedding mechanism. Usually, the set of instruction codes is known as the lifting plan. When the fabric weave and draft are decided, the lifting plan for weaving the fabric structure can then be generated automatically.

We have described the details of the automatic generation of lifting plans in our previous work [5]. Here, we have adopted the same principle for draft and lifting plan automatic generation because the orthogonal and angle-interlock structures have also been represented in the form of 2D binary matrices.

Weavers' Beam Calculation

In weaving 3D complex fabrics, it is usually the case that the warp ends are consumed at different rates according to the weave structure. It is necessary at times to use a number of weavers' beams for the warp supply. Correlating each warp end to a weavers' beam for a 3D complex fabric structure can be an extremely tedious and error-prone job. The CAD/CAM software provides the facility to calculate the minimum number of weavers' beams and correlate each warp end to a beam.

There are only three sets of warp yarns involved in an orthogonal structure—straight warp yarns, binding warp yarns, and inverse binding warp yarns. Straight warp yarns are subject to a different level of tension than the other two sets. Binding warp yarns and inverse binding warp yarns have opposite yarn paths in the fabric, but their yarn consumption rates are the same. Thus, a minimum number of two weavers' beams is sufficient for weaving the orthogonal structure.

In the case of the angle-interlock structure, there are two set of warp yarns at most—interlocking and non-interlocking. Each set of warp yarns is uniformly interlaced with weft yarns, and each set of warp yarns is exposed to the same level of tension. We can conclude that for the angle-interlock structure, at most, only one or two weavers' beams are needed, depending on the presence of the non-interlocking warp yarns.

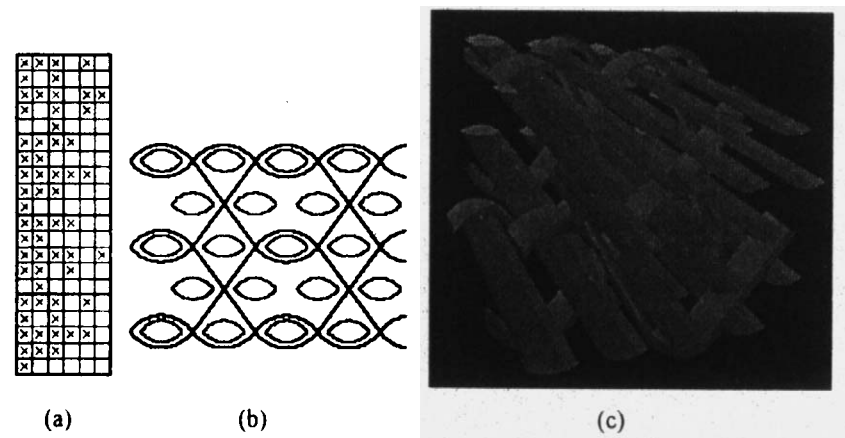

FIGURE 9. (a) The weave, (b) 2D, and (c) 3D representations of the *[5, 3]* angle-interlock structure.

Programming Implementation

We have written two Microsoft Windows-based programs to implement the models and algorithms described above for the orthogonal and angle-interlock woven structures. Both programs provide a user-friendly interface, shown in Figures 10a and 11a for the orthogonal and angle-interlock structures, respectively, to allow the user to input the necessary structural parameters. Once the structural information is provided, the programs take over and automatically generate the weaves, the results of which are shown in Figures 10b and 11b.

We have created draft and lifting plans for both kinds of 3D structures to facilitate the CAM of such structures. Figure 12 shows the automatically generated draft and lifting plan for weaving the enhanced orthogonal structure illustrated in Figure 10b. To help the users examine the structures, the programs also provide a function for viewing the cross sections of the structures. Cross-sectional views are illustrated in Figure 13. Furthermore, both orthogonal and angle-interlock structures have been visualized to provide 3D views of the structures, which will be useful in many ways, including evaluation of physical and mechanical properties of the structures. Figures 1 and 9c show the 3D views of the orthogonal and angle-interlock structures, respectively. Details in this regard will be discussed in the next section.

The interfaces of the programs use standard Windows convention and are therefore user-friendly. A file management facility is provided so that the user can save and load the weaves for archiving purposes. A weave can be copied into clipboard and used by other Windows applications supporting an OLE link (object linking and embedding), which is a method of sharing data between applications in Microsoft Windows.

Three-Dimensional Visualization

As mentioned earlier, both the orthogonal and angle-interlock 3D woven structures can be visualized in three dimensions. We have used VRML [1, 9] as a major tool for this development. Most 3-D graphics vendors and most web browser vendors, endorse VRML and it also shares a general concept of computer graphics. A VRML file is a text file containing the description of 3D objects and 3D environments, which are referred as the "world."

The space in the world can be specified by using the XYZ 3D coordinate system. The origin is the point through which the X, Y, and Z axes all pass. VRML assumes that, by default, the positive Y-axis points up, the positive X-axis points right, and the positive Z-axis points toward the user. The transformations that can happen in a 3D world are translation, rotation, and scaling. Translation moves an object from one point to another. Rotation rotates objects around the X-, Y-, or Z-axes. Scaling changes the size of objects. VRML 2.0 provides an extrusion technique that allows a cross section to be extruded along a spine. Cross sections and spines are defined with the 3D coordinate system.

The 3D image of a yarn can be created by specifying the yarn cross section and yarn path within the 3D woven

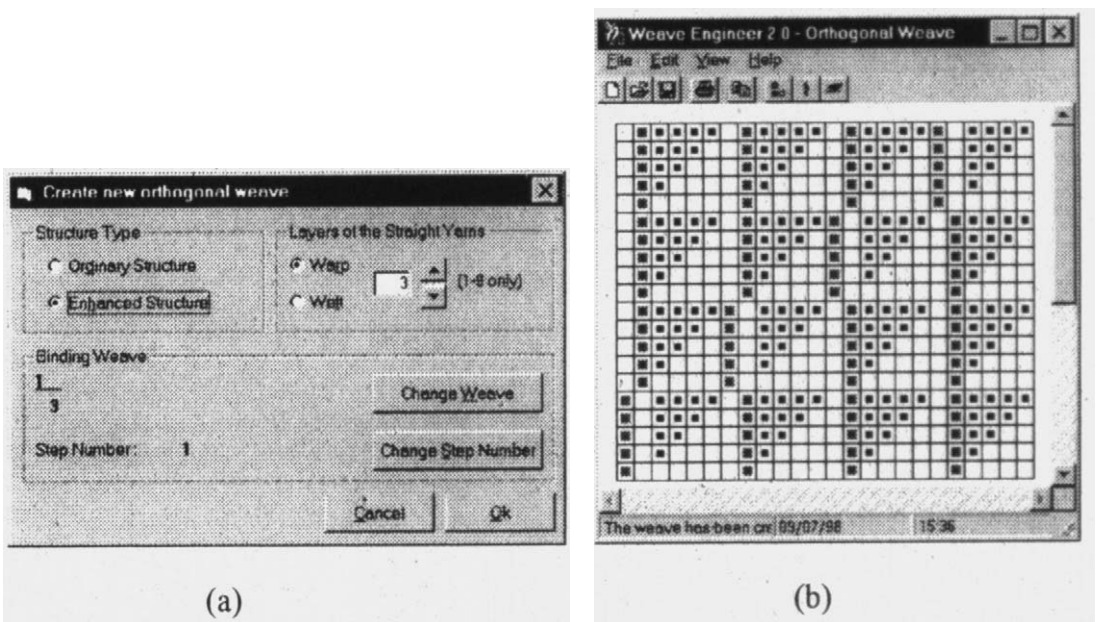

FIGURE 10. (a) Input interface for the orthogonal weaves and (b) the generated weave.

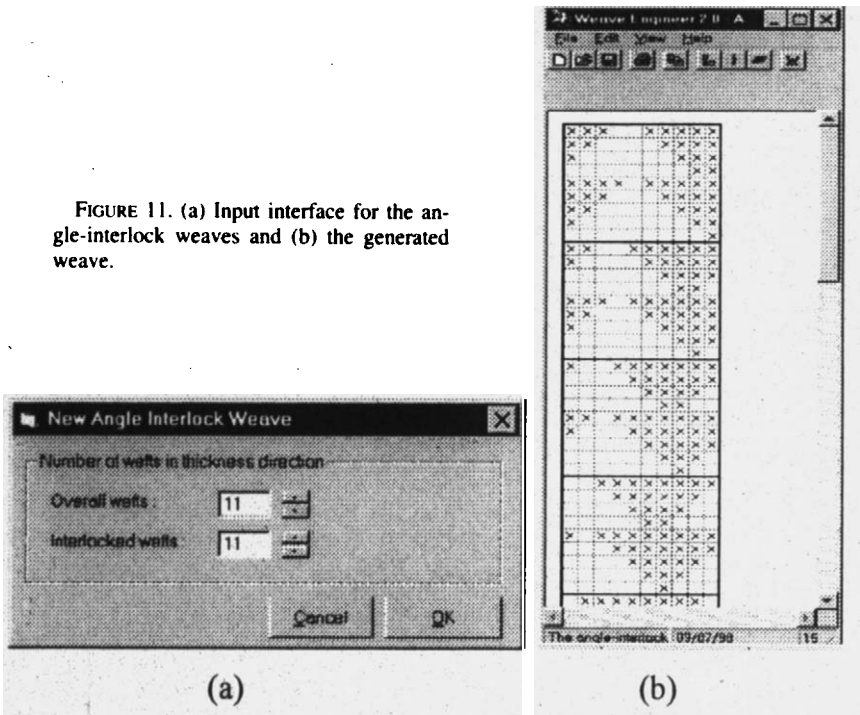

FIGURE 11. (a) Input interface for the angle-interlock weaves and (b) the generated weave.

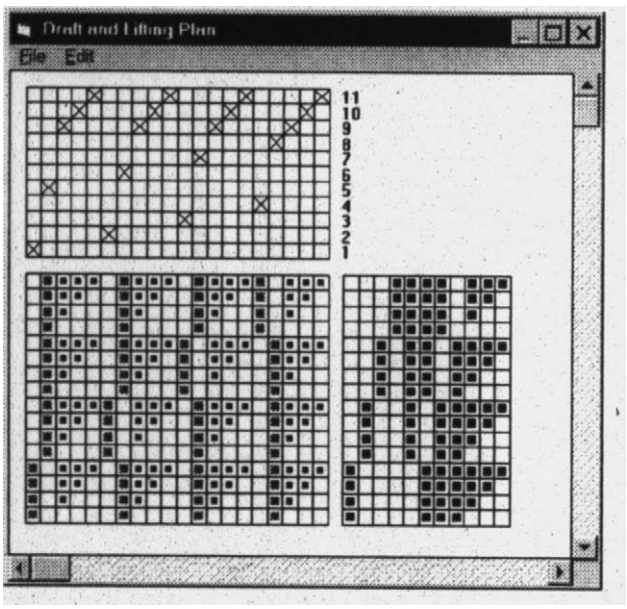

FIGURE 12. Window for draft and lifting plan.

structures. The image created for each component yarn is then transformed to the appropriate position. The 3D image of a complex woven structure is generated when the component yarns are assembled together.

In this work, the yarn cross section is assumed to be lenticular, as shown in Figure 14. A lenticular shape is formed by joining two identical arcs facing each other. If the width w and the height h of a lenticular shape are specified, the radius of the arc r can be calculated as follows [4]:

$$r = (w^2 + h^2)/(4h) \quad . \tag{14}$$

In order to generate an arc, we use the following parametric representation of an origin-centered circle [11]:

$$x = 5 \cos \theta \tag{15}$$

and

$$y = r \sin \theta \tag{16}$$

for $0 \leq \theta \leq \pi$. At any point on an origin-centered circle,

$$\begin{aligned} x_{i+1} &= r \cos (\theta_i + \Delta\theta) \\ &= r(\cos \theta_i \cos \Delta\theta - \sin \theta_i \sin \Delta\theta) \end{aligned} \tag{17}$$

and

$$\begin{aligned} y_{i+1} &= r \sin (\theta_i + \Delta\theta) \\ &= r(\cos \theta_i \sin \Delta\theta + \sin \theta_i \cos \Delta\theta) \quad , \end{aligned} \tag{18}$$

where θ_i is the value of the angle that yields the point at (s_i, y_i). Substituting Equations 15 and 16 into Equations 17 and 18, respectively, leads to

$$x_{i+1} = x_i \cos \Delta\theta - y_i \sin \Delta\theta \tag{19}$$

and

$$y_{i+1} = x_i \sin \Delta\theta + y_i \cos \Delta\theta \quad . \tag{20}$$

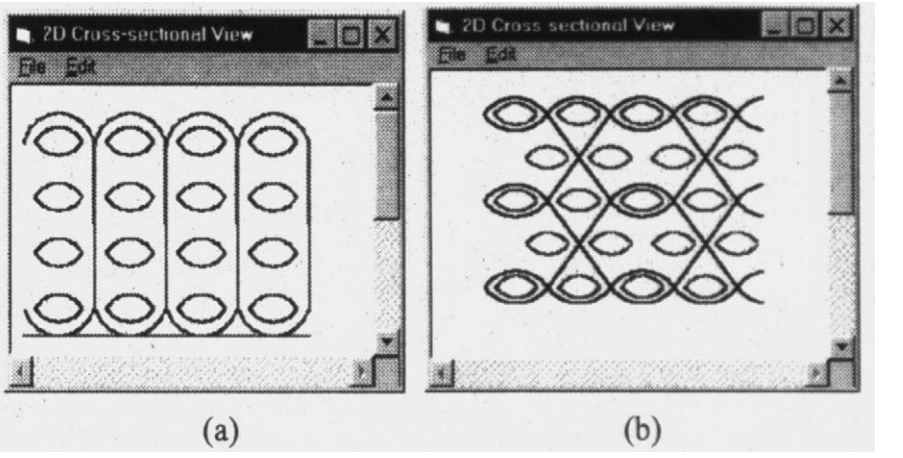

FIGURE 13. Cross-sectional views of (a) an orthogonal structure and (b) an angle-interlock structure.

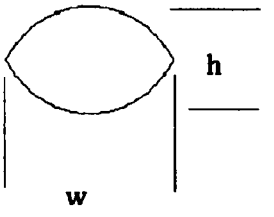

FIGURE 14. Lenticular cross section.

If n is the number of uniformly spaced points on a circle, $\Delta\theta$ is then equal to $2\pi/(n-1)$. A circle is plotted when varying i from 1 to $n+1$. An arc can be created by using a limited range of i. When the programs receive the request to generate the 3D image of a weave structure, the weave data calculated previously are used to generate a VRML file. The VRML viewer program is then invoked to show the 3d image described by the VRML file. The 3D image is able to be moved, rotated, and zoomed in and out using tools provided to the viewer.

Conclusions

We have discussed the CAD/CAM of two kinds of complex 3D woven structures, *i.e.*, orthogonal and angle-interlock. As result, weaves for both structures are successfully described as mathematical functions, making their automatic generation possible. Two Windows-based applications written in Visual Basic 5 implement the models and algorithms, leading to two programs useful for the CAD/CAM of the orthogonal and angle-interlock structures. The applications can also visualize the structures in both 2D and 3D fashion.

Literature Cited

1. Ames, A. L., Nadeau, D. R., and Moreland, J. L., VRML 2.0 Source Book, 2nd ed., Wiley, Toronto, 1996.
2. Byun, J. H., and Chou, T. W., Elastic Properties of Three-dimensional Angle-interlock Fabric Preforms, *J. Textile Inst.* **81**(4), 538 (1990).
3. Chen, X., Knox, R. T., McKenna, D. F., and Mather, R. R., Automatic Generation of Weaves for CAM of 2D and 3D Woven Textile Structures, *J. Textile Inst.* **87**(2) Part 1, 356 (1996).
4. Chen, X., Knox, R. T., McKenna, D. F., and Mather, R. R., Solid Modelling and Integrated Manufacturing of Textile Interlinking Structures, in "Proc. Int. Conf.: Design to Manufacture in Modern Industry," Part 2, Bled-Slovenia, 1993, p. 682.
5. Chen, X., and Potiyaraj, P., CAD/CAM for Complex Woven Fabrics, Part I: Backed Cloths, *J. Textile Inst.* **89**(3) Part 1, 532 (1998).
6. Chen, X., and Potiyaraj, P., CAD/CAM for Complex Woven Fabrics, Part II: Multi-layer Fabrics, *J. Textile Inst.* **90**(1) Part 1, 73–90 (1999).
7. Goerner, D., "Woven Structure and Design: Part 2 Compound Structures," British Textiles Technology Group, Leeds, 1989.
8. Grosicki, Z. J., "Watson's Advanced Textile Design," 4th ed., Butterworth, London, 1977.
9. Netscape Communications Corp., Beginner's Guide to VRML, http://www.netscape.com/eng/live3d/howto, 1996.
10. Potiyaraj, P., and Chen, X., An Innovative Software System for Complex Woven Structures, in "Proc. 78th World Conference of the Textile Institute," Thessaloniki, Greece, 1997, vol. 3, p. 245.
11. Rogers, D. F., and Adams, J. A., "Mathematical Elements for Computer Graphics," 2nd ed., McGraw Hill, NY, 1990.

Manuscript received May 27, 1998; accepted July 23, 1998.